Chemistry–A European Journal
Research Article
doi.org/10.1002/chem.202203583
Chemistry Europe
European Chemical Societies Publishing
www.chemeurj.org

Fully Tin-Coated Coinage Metal Ions: A Pincer-Type Bis-stannylene Ligand for Exclusive Tetrahedral Complexation

Frederic Krätschmer,[a] Xiaofei Sun,[a] Sebastian Gillhuber,[a] Hannes Kucher,[a] Yannick J. Franzke,[b] Florian Weigend,[b] and Peter W. Roesky*[a]

Dedicated to Professor Hongjian Sun on the occasion of his 60th birthday.

Abstract: The synthesis of a novel bis-stannylene pincer ligand and its complexation with coinage metals (Cu^{I}, Ag^{I} and Au^{I}) are described. All coinage metal centres are in tetrahedral coordination environments in the solid state and are exclusively coordinated by four neutral Sn^{II} donors. ^{119}Sn NMR provided information about the behaviour in solution. All of the isolated compounds have photoluminescent properties, and these were investigated at low and elevated temperatures. Compared to the free bis-stannylene ligand, coordination to coinage metals led to an increase in the luminescence intensity. The new compounds were investigated in detail through all-electron relativistic density functional theory (DFT) calculations.

Introduction

The chemistry of coinage metals is of great interest due to their catalytic abilities, their luminescence properties, for example in OLEDs, and their ability to undergo metallophilic interactions.[1] Therefore, a great number of compounds comprising different types of ligand frameworks and donor atoms leading to various coordination modes are known in the literature.[2] While Cu^{I} prefers tetrahedral coordination with hard donors, Au^{I} compounds prefer linear arrangements with softer donor ligands, in agreement with Pearson's hard and soft acids and bases concept (HSAB).[3] Ag^{I} can be categorised in-between these two. Although Au^{I} prefers the linear coordination mode, there are many known tetrahedral Au^{I} complexes, using for example phosphine ligands.[4] In the case of neutral group 14 donor ligands, there are many known tetrylene complexes of the coinage metals with linear coordination geometry.[5] Recently, Khan and co-workers reported the reactions of structurally identical mono-silylene and -stannylene toward $[Ag^{I}SbF_6]$. Although in both cases ion pairs $[L_2Ag^{I}][SbF_6]$ (L = $[PhC(NtBu)_2EN(SiMe_3)_2]$, E = Si^{II}, Sn^{II}) are formed, remarkable differences were observed in their molecular structures. In the case of silylene, the Ag^{I} cation is linearly coordinated, whereas a bent Sn–Ag–Sn motif is observed for the stannylene, which is accompanied by additional weak coordination of F atoms of the counter anion. This shows that the heavier stannylene ligand can promote a more tetrahedral-like coordination environment.[6] The coordination of four heavier tetrylenes to a monocationic coinage metal centre is rare. Best to our knowledge, there is only one example in which a Cu^{I} centre is tetrahedrally coordinated by four stannylenes.[7]

The large ionic radius of Sn^{II} makes it a softer base compared to the lighter tetrylenes, thus making it ideal for the coordination of Au^{I}. Meanwhile, due to the chelating ability of the pincer, it is also capable of coordinating Ag^{I} and Cu^{I} in a similar manner. We report on the synthesis, characterisation, and luminescence properties of a novel pincer-type bis-stannylene ligand (**SnNSn**) and three coinage metal complexes (**1**–**3**) stabilized by four stannylene moieties where the coinage metals present exclusive tetrahedral coordination geometries. To rationalise the findings, quantum chemical calculations at density functional theory (DFT) level were performed with the program suite TURBOMOLE.[8] Complete computational details are given within the Supporting Information.

Results and Discussion

The 2,6-diaminopyridine-bridged bis-stannylene **SnNSn** was prepared in a straightforward synthesis, similar to the analogue bis-silylene species reported by Driess (Scheme 1).[9] Deprotonation of 2,6-di(ethylamino)pyridine by *n*-BuLi and subsequent reaction with two equivalents of chlorostannylene $[L^{Ph}Sn^{II}Cl]$ (L^{Ph} = $PhC(NtBu)_2$) led to the formation of the bis-stannylene **SnNSn**. Extraction with *n*-pentane and storage overnight at

[a] F. Krätschmer, Dr. X. Sun, S. Gillhuber, H. Kucher, Prof. Dr. P. W. Roesky
Institute of Inorganic Chemistry
Karlsruhe Institute of Technology
Engesserstr. 15, 76131 Karlsruhe (Germany)
E-mail: roesky@kit.edu
Homepage: https://www.aoc.kit.edu/AK%20Roesky.php
[b] Dr. Y. J. Franzke, Prof. Dr. F. Weigend
Fachbereich Chemie, Philipps-Universität Marburg
Hans-Meerwein-Str. 4,35032 Marburg (Germany)

Supporting information for this article is available on the WWW under https://doi.org/10.1002/chem.202203583

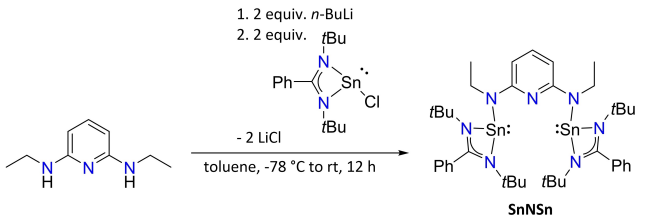

Scheme 1. Synthesis of **SnNSn**.

−30 °C gave the analytically pure product as yellow crystalline solid in 54% yield.

Single crystals suitable for X-ray diffraction analysis were obtained by slow evaporation of toluene at room temperature. **SnNSn** crystallises in the monoclinic space group $P2_1/c$ and its solid-state molecular structure is shown in Figure 1. In contrast to the molecular structure of the analogue bis-silylene in the solid state,[9] in which both silylene moieties are directed away from each other, the stannylene subunits in **SnNSn** are oriented towards each other with a Sn1···Sn2 distance of 3.7622(5) Å.[10] Geometry optimisation at the PBE0/def2-TZVP level[11, 12] (further information given in the Supporting Information) results in a Sn···Sn distance of 3.736 Å which fits well with the experimental data (3.762(3) Å). As already indicated by this large Sn–Sn distance, the compound can rather be described as a bis(stannylene) consisting of two isolated stannylene units than a distannene featuring significant covalent bonding contributions between the Sn^{II} atoms.

In accordance with this, localisation according to the Foster-Boys method[13] gave no orbital with substantial contributions between the two Sn^{II} atoms and the Wiberg bond index (WBI) amounts to only 0.12. Further, inspection of the electron density does not provide any indication of a chemical bond. In the middle between the two Sn^{II} atoms this quantity amounts to 0.0111 a.u. (for a plot see Figure S30 in the Supporting Information). This is almost identical to twice the electron density of an isolated Sn^{II} atom 1.868 Å (half of the calculated Sn–Sn distance in **SnNSn**) away from the nucleus (0.0106 a.u.). For a typical Sn–Sn single bond, for example, in Sn_2H_6, in contrast, corresponding treatments result in a WBI close to one (0.89) and a density at the bond centre that is much higher than the sum of two isolated atoms. This is true for both the Sn–Sn equilibrium distance in Sn_2H_6 (2.770 Å), and for the Sn–Sn distance increased to that in **SnNSn**, for which 0.0198 a.u. at the bond centre is obtained, about 80% more than in **SnNSn**. Similar to the situation in previously described bis(stannylene) ligands, the canonical molecular orbitals resemble the combinations of two isolated stannylene fragment orbitals as shown in Figure 2. The HOMO-3 and HOMO-1 can be regarded as in-phase and out-of-phase combinations of stannylene lone pairs, respectively.[14]

In agreement with the solid-state structure, only one signal was observed in the ^{119}Sn NMR spectrum at −136.0 ppm, which is upfield-shifted compared to the chlorostannylene (29.6 ppm) and comparable to literature known bis(stannylenes).[15] Despite the long Sn–Sn distance, the presence of isotope satellites due to ^{119}Sn–^{117}Sn coupling ($^1J_{119Sn\text{-}117Sn} = 4087$ Hz) indicates an interaction between the two Sn^{II} atoms. Notably, this significant coupling is present despite there is no indication for a chemical bond. A similar coupling interaction has been reported in a xanthene-bridged bis-stannylene compound, which exhibits a Sn···Sn distance of 3.0009(7) Å.[14] Calculations of the $^1J_{119Sn\text{-}117Sn}$ coupling constant at the spin-orbit exact-two-component[16] (X2C) level of theory with different density functionals (BH&HLYP,[17] cTPSSh,[18] PBE0,[11] ωB97X-D,[19] cTMHF[20]) and tailored x2c-TZVPall-2c basis sets[21] resemble the experimentally observed value of 4087 Hz (Tables S8–S11). Detailed investigations of the coupling mechanism reveal that it can best be described as through-space coupling between the Sn^{II} atoms which can be fine-tuned by ligand-design (see the Supporting Information). The ^{119}Sn NMR shifts calculated at the same levels also resemble the measured value of −136 ppm.[16d, e] However, analogous calculations of the ^{119}Sn NMR shift using the scalar-relativistic X2C ansatz[16c] show significant deviations from this value (Table S8). This reveals that spin-orbit coupling plays a crucial role for an adequate description of the ^{119}Sn NMR properties of **SnNSn**. However, the Sn–Sn bonding and geometric structure are well described with the scalar-relativistic approximation using both the effective core potential (ECP) or the all-electron approach.

Having the bis-stannylene at hand, we were particularly interested in the reaction with suitable coinage metal precursors. Reaction of **SnNSn** with [$Cu^I(C_6F_5)$·dioxane], [$Ag^I(C_6F_5)$·MeCN] and [$Au^I(C_6F_5)$·tht] (tht = tetrahydrothiophene) were carried out in toluene, and the corresponding ionic

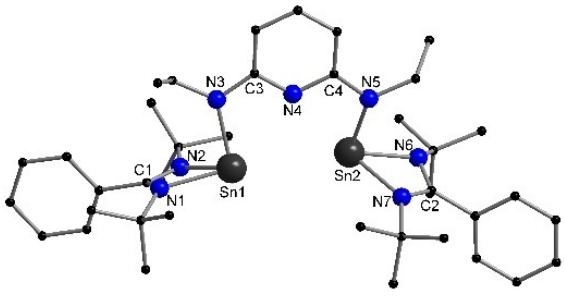

Figure 1. Molecular structure of **SnNSn**. Hydrogen atoms are omitted for clarity. Only one position for the disordered *t*Bu and Et groups is depicted for clarity. Selected distances [Å] and angles [°]: Sn1···Sn2 3.7622(5), Sn1–N1 2.237(3), Sn1–N2 2.214(3), Sn1–N3 2.132(3), Sn2–N5 2.109(3), Sn2–N6 2.238(3), Sn2–N7 2.207(3); N1–Sn1–N2 59.39(10), N6–Sn2–N7 59.32(12).

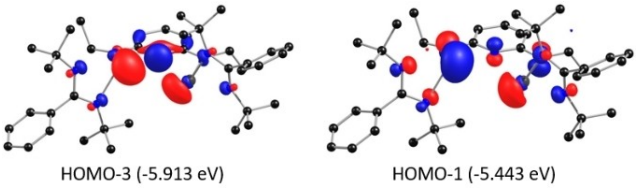

Figure 2. HOMO-3 (left) and HOMO-1 (right) of **SnNSn**. Contours are drawn at 0.06 atomic units. Colours: C black, N blue, Sn grey. Hydrogen atoms were omitted for clarity.

complexes [(**SnNSn**)$_2$M][M(C$_6$F$_5$)$_2$] (M = **1**: Cu^I; **2**: Ag^I; **3**: Au^I) were obtained (Scheme 2). All three complexes were isolated as yellow crystalline solids in moderate to good yields (**1**: 47%; **2**: 61%; **3**: 81%).

The Ag^I complex **2** crystallises in the triclinic space group $P\bar{1}$, whereas the Cu^I and Au^I compounds **1** and **3** are isomorphous, both crystallising in the monoclinic space group $C2/c$. Interestingly, two different coordination geometries are realised for the same metal in the ionic species **1**–**3**.

In the cationic part, the central coinage metal M$^+$ is coordinated by four Sn^{II} atoms of two bis-stannylene ligands, adopting a slightly distorted tetrahedral geometry with Sn–M–Sn angles of 100–120° (Figure 3). Similar coordination geometries with bis-stannylene ligands have been found for the other d^{10} metals Ni^0 and Pt^0 in the work of Hahn and co-workers.[22] The counter-anions of the ion pairs **1**–**3** are the linearly coordinated anions [M(C$_6$F$_5$)$_2$]$^-$ (M = **1**: Cu^I; **2**: Ag^I; **3**: Au^I). There is a clear cation-anion separation in the solid state with no significant interaction. A rearrangement of one of the C$_6$F$_5$ groups leading to the linear [M(C$_6$F$_5$)$_2$]$^-$ anions seems to be one of the driving forces for the reaction. For control, mesityl-Cu^I or -Ag^I were treated with **SnNSn** and no visible reaction was seen according to NMR spectroscopy, leading to the conclusion that the formation of the counter-anion [M(C$_6$F$_5$)$_2$]$^-$ must be crucial for the complexation.

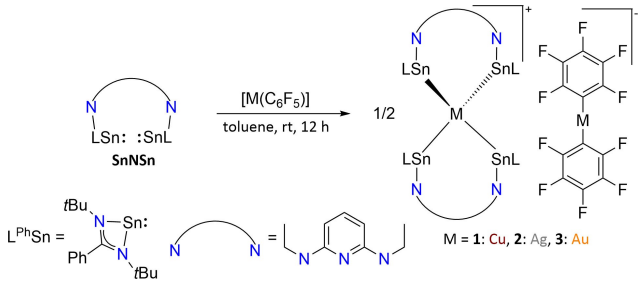

Scheme 2. Synthesis of coinage metal bis-stannylene compounds **1**–**3**.

In the cation, the separation between the central metal and the pyridine nitrogen atom of more than 3.5 Å excludes any bonding interactions. The Sn^{II}–M bond lengths within each compound are almost identical (Table S3) and all Sn^{II}–M bond lengths (avg.: **1**: 2.5183 Å; **2**: 2.6689 Å; **3**: 2.5893 Å) are in accordance with known examples of coinage metal stannylene complexes.[6–7,23] Most strikingly, the Sn^{II}–Ag^I distance is the longest within this series. The shorter Sn^{II}–Au^I bond lengths compared to Sn^{II}–Ag^I reflect scalar-relativistic effects of Au^I. The structural parameters could be well reproduced by quantum chemical calculations. The Sn^{II}–M^I distances are consistently overestimated by ~0.1 Å, thus resembling the experimental trend regarding the Sn–M^I bond lengths (Cu^I < Au^I < Ag^I; Table S4). The fact that the Sn^{II}–Au^I bond is shorter than the Sn^{II}–Ag^I bond is due to scalar-relativistic effects. Their neglection in a non-relativistic optimisation of complex **3** leads to an increase in the Sn^{II}–Au^I bond length of 0.16 Å and thus to Sn^{II}–M^I distances increasing from Cu^I over Ag^I to Au^I. Coordinates of the optimized structures (optimized-structures.txt) as well as the non-relativistic basis (nonrelativistic-basis-set.txt) are given in separate ASCII files as part of the Supporting Information. Natural population analysis[24] (NPA) charges on the coinage metal centres reflect the trends observed for the bond lengths. While the calculated NPA charge increases when going from Cu^I (0.31) to Ag^I (0.41), indicating less saturation of the positive charge due to the Sn^{II} atoms of the ligands, it decreases again when going on to Au^I (0.20). Like for the bond lengths, this trend inversion is a consequence of scalar relativity. Without its consideration one gets an NPA charge of 0.49 for Au^I.

Coinage metal stannylene complexes are still in their infancy and to the best of our knowledge, compounds **2** and **3** are the first structurally characterised Ag^I and Au^I complexes exclusively coordinated by four Sn^{II} substituents. The Sn^{II}–M^I bonding situation in the coinage metal complexes **1**–**3** can best be described as saturation of the positive charge of the M centre (M^I = Cu^I, Ag^I, Au^I) by donation of electron density from

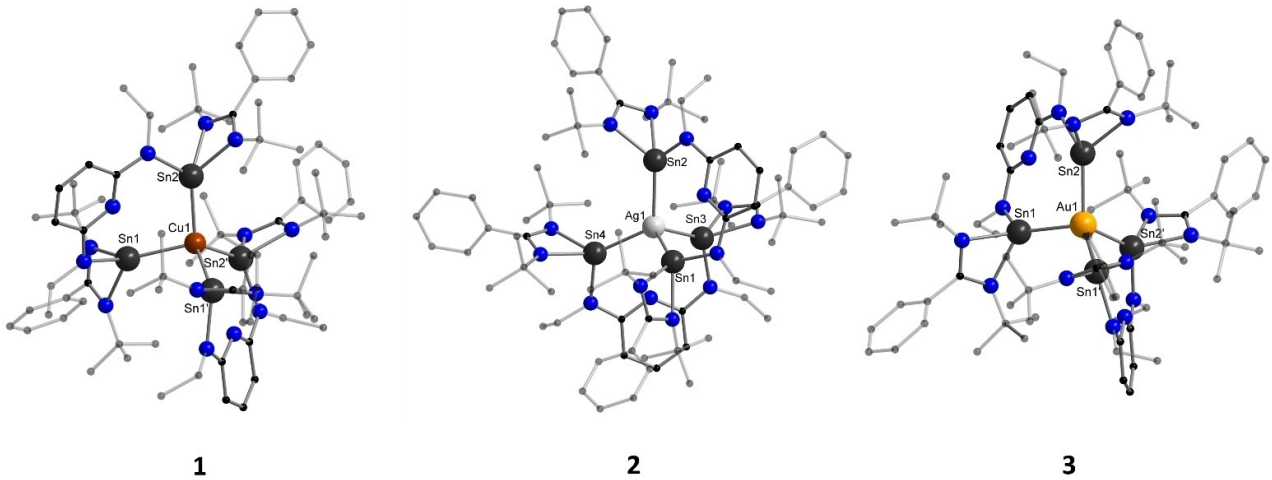

Figure 3. Solid-state molecular structure of compounds **1**–**3**. Hydrogen atoms; solvent and counter ions are omitted for clarity. Detailed bond lengths and angles are provided in the Supporting Information.

the Sn^{II} atoms of the bis-stannylene ligand. Minimisation of electrostatic repulsion between the Sn^{II} atoms then rationalises the tetrahedral coordination geometry observed for all three compounds **1**–**3**. Foster-Boys localisation[13] for **1**–**3** gave in each case four localised molecular orbitals (LMOs) representing the four individual Sn^{II}–M interactions (Figures S31–S33). Mulliken population analyses[25] of these LMOs (Tables S5–S7) reveal that they are mainly centred on the Sn^{II} atoms, thus supporting the above made hypothesis that charge delocalisation mainly occurs from the Sn^{II} atoms to the cationic coinage metal centres.

The ^{1}H NMR spectra of compounds **1**–**3** resemble each other and only one signal is detected for all *t*Bu groups in each. In the ^{13}C NMR spectra the NCN signal of the amidinate ligand in **SnNSn** appears at 171.3 ppm.[26] The resonances in the coinage metal compounds are downfield shifted (**1**: 174.5 ppm; **2**: 174.2 ppm; **3**: 173.8 ppm). In the ^{119}Sn NMR spectrum of Cu^{I} complex **1**, a singlet was detected at −105.9 ppm at 193 K. For the Ag^{I} complex **2**, the ^{119}Sn NMR spectrum shows a broad doublet at 80.9 ppm due to coupling with the Ag^{I} isotopes ($\nu_{1/2}$ = 425 Hz, $^{1}J_{^{119}Sn\text{-}^{107/109}Ag}$ = 1620 Hz). The Sn^{II}–Ag^{I} coupling in the tetra-stannylene species **2** is considerably weaker than that found in mono-stannylene Ag^{I} species (2600–4600 Hz).[27] In contrast, the ^{119}Sn NMR spectrum of the Au^{I} complex **3** reveals two broad singlets (99.7 and 29.5 ppm) with visible ^{117}Sn satellites ($^{2}J_{^{119}Sn\text{-}^{117}Sn}$ ≈3200 Hz) indicating the presence of two different types of Sn nuclei in solution.

Calculations of chemical shifts and coupling constants of **1**, **2** and **3** at the X2C level of theory using different density functional approximations were carried out (see the Supporting Information). For compounds **1** and **2**, we observe a very good agreement of theory and experiment, while for compound **3** qualitative discrepancies were obtained. For the latter, the calculations show only one resonance and also the experimental coupling constant is not well reproduced. This observation gives evidence that the structure of compound **3** in solution does not retain the tetrahedral geometry found in both the solid state and the quantum chemical studies. Presumably, one of the Sn^{II} atoms (99.7 ppm) in the bis-stannylene ligand is closer coordinated to the metal centre than the other one (29.5 ppm). All signals are strongly downfield-shifted compared to the free ligand (−136.0 ppm).

Photoluminescence spectra of all compounds were measured at variable temperatures from 9 K to room temperature. To the best of our knowledge, this is the first investigation of luminescence properties of bis-tetrylene species. The compounds are yellow to orange in colour and show an orange to red luminescence at low temperatures under excitation at 360 nm (Figure 4). Figures 5 and 6 show the photoluminescence excitation (PLE) and photoluminescence emission (PL) spectra of **SnNSn** and compounds **1**–**3**. A strong decrease in luminescence intensity with increasing temperature is observed. At room temperature, only weak luminescence can be observed. The PL spectra of **SnNSn** show a strong dependence on the excitation wavelength resulting in two different spectra (Figure 4). Excitation at short wavelengths (260 nm) leads to a weak band at 500 nm and a strong one at 730 nm which is changing

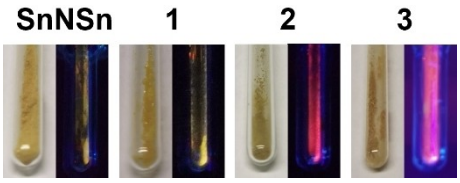

Figure 4. Compounds **SnNSn**, **1**–**3** left: daylight (293 K), right: at 360 nm (77 K).

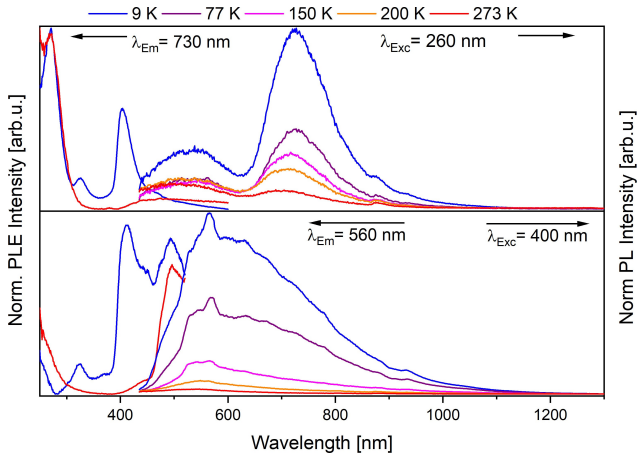

Figure 5. Solid-state photoluminescence emission (PL) and excitation (PLE) spectra of **SnNSn** at different temperatures, measured at various wavelengths showing different PL behaviour. The PL and PLE spectra were excited/ recorded at the indicated wavelengths.

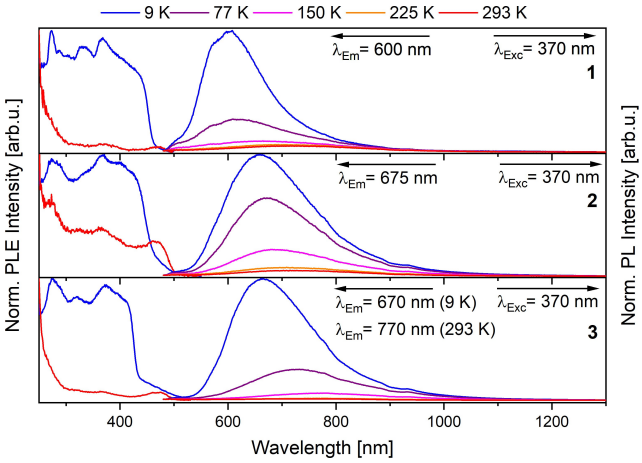

Figure 6. Solid-state photoluminescence emission (PL) and excitation (PLE) spectra of compounds **1**–**3** at different temperatures.

at elevated temperatures. Excitation at 400 nm results in a broad unsymmetric band, with its maximum at 566 nm. The PL emission in both spectra depicted in Figure 4 ranges far in the near-infrared (NIR) region (up to 1200 nm).

The spectra of compounds **1**–**3** resemble each other, all showing a broad band ranging into the NIR region. The PLE onset of **1** and **2** at 9 K is around 460 nm, while it is 430 nm for

compound **3**. The Cu^{I} compound **1** shows a band at 608 nm, while the emission maxima of **2** and **3** are red-shifted to around 660 nm at 9 K. At 77 K, the Au^{I} compound **3** experiences a major redshift to 731 nm which gets even more pronounced at elevated temperatures. Overall, Cu^{I} compound **1** is blue-shifted in comparison to the higher homologues of group 11, whereas usually a strong red-shift can be observed.[28] The excited state lifetimes are in the range of microseconds, hence indicating phosphorescent processes, having lifetimes from 5 to 8 μs at room temperature extending to 10 to 15 μs at 77 K. At low temperatures, the decay processes of **SnNSn** and compound **1** are more complicated and show a second, longer lifetime of 217 μs (**SnNSn**) and 75 μs (**1**).

To gain a deeper insight into the photoluminescence properties of the free ligand **SnNSn** as well as compounds **1**–**3**, time-dependent density functional theory (TDDFT) calculations[29] were performed at level PBE0/def2-TZVP.[11, 12] Singlet vertical excitation energies for the six lowest lying excitations were calculated for all compounds (Tables S19–S22). Visual inspection of the difference between the non-relaxed density of the excited state and the ground state of the free ligand **SnNSn** reveals that excitation mainly occurs from the π-system of the pyridine ring and the adjacent N atoms to the π-system of the phenyl groups and, to a lesser extent, the two Sn^{II} atoms (Figure S36). The same holds for the coinage metal complexes **1**–**3**. For these, additional metal-centred transitions can be observed at higher energies (Figures S37–S39). To shed light on the phosphorescence emission process, the structure of the lowest excited triplet state of each compound was optimized using scalar-relativistic TDDFT gradients.[29a,30] The phosphorescence emission properties were then investigated in an indirect manner by calculating the lowest vertical excitation energy from the singlet to the triplet state for the so obtained triplet geometry. In all cases, the lowest lying (de)excitation corresponds to a HOMO-LUMO transition (Table S23). For **SnNSn**, the HOMO still corresponds to the pyridine π-system and the adjacent N atoms (similar to the situation in the singlet ground state structures), while the LUMO now corresponds to p-type orbitals on the Sn^{II} atoms (Figures S40 and S41). Thus, the phosphorescence process in the free ligand can best be described as deexcitation from Sn^{II} p-orbitals to the π-system of the pyridine ring as well as its neighbouring N atoms. Similar to the free ligand, the HOMOs in **1**–**3** correspond to the π-system of a pyridine moiety and the N atoms attached to it. Mulliken population analyses[25] of the LUMOs of **1**–**3** revealed contributions from the Sn^{II} atoms as well as the central coinage metal (Tables S27, S29, and S31). Consequently, the electronic situation on the Sn^{II} atoms plays a crucial role for the phosphorescence emission properties and rationalises the influence of metal coordination found for compounds **1**–**3**. The experimentally observed red shift in the phosphorescence emission when going from Cu^{I} over Ag^{I} to Au^{I} is qualitatively reproduced by the calculations (Table S23) and can mainly be attributed to the influence of the metal on the LUMO energy in the complexes. The anion does not contribute to the luminescence properties, in agreement with the literature.[31]

Conclusions

The pincer-type bis-stannylene **SnNSn** has been synthesised and fully characterised. The molecular structure in the solid state and the NMR spectra showed a weak interaction between the two Sn^{II} atoms. This was further investigated by quantum chemical calculations. Reaction with coinage metal precursors led to the formation of three complexes with a single Cu^{I} (**1**), Ag^{I} (**2**) or Au^{I} (**3**) centre, tetrahedrally coordinated by four stannylene moieties. NMR studies revealed that Au^{I} compound **3** presumably does not retain its solid-state structure in solution. Photoluminescence studies were performed for all compounds and show broad bands tailing far into the NIR region.

Experimental Section

See the Supporting Information for the synthesis and characterisation of all compounds, the NMR, IR and PL spectra, as well as X-ray crystallography and DFT calculation details.

Deposition Numbers 2220031 (for **SnNSn**), 2220032 (for **1**), 2220033 (for **2**), and 2220034 (for **3**) contain the supplementary crystallographic data for this paper. These data are provided free of charge by the joint Cambridge Crystallographic Data Centre and Fachinformationszentrum Karlsruhe Access Structures service.

Acknowledgements

Financial support from the DFG-funded transregional collaborative research centre SFB/TRR 88 "Cooperative Effects in Homo and Heterometallic Complexes (3MET)" is gratefully acknowledged (project C1). S.G. thanks the Fonds der Chemischen Industrie for the generous fellowship (no. 110160). Dr. Sergei Lebedkin, KIT, is acknowledged for helpful support. Open Access funding enabled and organized by Projekt DEAL.

Conflict of Interest

The authors declare no conflict of interest.

Data Availability Statement

The data that support the findings of this study are available in the supplementary material of this article.

Keywords: coinage metals · luminescence · pincers · stannylene · tetrahedra

[1] a) V. W.-W. Yam, V. K.-M. Au, S. Y.-L. Leung, *Chem. Rev.* **2015**, *115*, 7589–7728; b) S. Raju, H. B. Singh, R. J. Butcher, *Dalton Trans.* **2020**, *49*, 9099–9117; c) H. Schmidbaur, A. Schier, *Chem. Soc. Rev.* **2012**, *41*, 370–412; d) F. Scherbaum, A. Grohmann, G. Müller, H. Schmidbaur, *Angew. Chem. Int. Ed.* **1989**, *28*, 463–465; *Angew. Chem.* **1989**, *101*, 464–466; e) H. Schmidbaur, *Gold Bull.* **1990**, *23*, 11–21; f) M. Jansen, *Angew. Chem. Int.*

Ed. **1987**, *26*, 1098–1110; *Angew. Chem.* **1987**, *99*, 1136–1149; g) N. V. S. Harisomayajula, S. Makovetskyi, Y.-C. Tsai, *Chem. Eur. J.* **2019**, *25*, 8936–8954; h) H. L. Hermann, G. Boche, P. Schwerdtfeger, *Chem. Eur. J.* **2001**, *7*, 5333–5342; i) H. Schmidbaur, A. Schier, *Angew. Chem. Int. Ed.* **2015**, *54*, 746–784; *Angew. Chem.* **2015**, *127*, 756–797; j) M. Jansen, *J. Less-Common Met.* **1980**, *76*, 285–292.

[2] a) V. R. Naina, F. Krätschmer, P. W. Roesky, *Chem. Commun.* **2022**, *58*, 5332–5346; b) A. A. Mohamed, *Coord. Chem. Rev.* **2010**, *254*, 1918–1947; c) P. D. Akrivos, H. J. Katsikis, A. Koumoutsi, *Coord. Chem. Rev.* **1997**, *167*, 95–204; d) J. C. Y. Lin, R. T. W. Huang, C. S. Lee, A. Bhattacharyya, W. S. Hwang, I. J. B. Lin, *Chem. Rev.* **2009**, *109*, 3561–3598.

[3] a) R. G. Pearson, *J. Chem. Educ.* **1968**, *45*, 643; b) R. G. Pearson, *Inorg. Chim. Acta* **1995**, *240*, 93–98.

[4] a) M. Osawa, I. Kawata, S. Igawa, A. Tsuboyama, D. Hashizume, M. Hoshino, *Eur. J. Inorg. Chem.* **2009**, 3708–3711; b) M. Osawa, I. Kawata, S. Igawa, M. Hoshino, T. Fukunaga, D. Hashizume, *Chem. Eur. J.* **2010**, *16*, 12114–12126; c) A. Pintado-Alba, H. de la Riva, M. Nieuwhuyzen, D. Bautista, P. R. Raithby, H. A. Sparkes, S. J. Teat, J. M. Lopez-de-Luzuriaga, M. C. Lagunas, *Dalton Trans.* **2004**, 3459–3467; d) S. J. Berners-Price, P. J. Sadler, *Inorg. Chem.* **1986**, *25*, 3822–3827; e) P. A. Bates, J. M. Waters, *Inorg. Chim. Acta* **1984**, *81*, 151–156.

[5] a) C. Kaub, S. Lebedkin, A. Li, S. V. Kruppa, P. H. Strebert, M. M. Kappes, C. Riehn, P. W. Roesky, *Chem. Eur. J.* **2018**, *24*, 6094–6104; b) T. Simler, K. Möbius, K. Müller, T. J. Feuerstein, M. T. Gamer, S. Lebedkin, M. M. Kappes, P. W. Roesky, *Organometallics* **2019**, *38*, 3649–3661; c) M. Ghosh, N. Sen, S. Khan, *ACS Omega* **2022**, *7*, 6449–6454; d) S. Abe, Y. Inagawa, R. Kobayashi, S. Ishida, T. Iwamoto, *Organometallics* **2022**, *41*, 874–882; e) P. Chibde, R. K. Raut, V. Kumar, R. Deb, R. Gonnade, M. Majumdar, *Chem. Asian J.* **2021**; f) M. Walewska, J. Hlina, W. Gaderbauer, H. Wagner, J. Baumgartner, C. Marschner, *Z. Anorg. Allg. Chem.* **2016**, *642*, 1304–1313.

[6] N. Parvin, R. Dasgupta, S. Pal, S. S. Sen, S. Khan, *Dalton Trans.* **2017**, *46*, 6528–6532.

[7] J. K. West, G. L. Fondong, B. C. Noll, L. Stahl, *Dalton Trans.* **2013**, *42*, 3835–3842.

[8] a) in *TURBOMOLE V7.7 2022*, a development of University of Karlsruhe and Forschungszentrum Karlsruhe GmbH, 1989–2007, TURBOMOLE GmbH, since 2007; b) S. G. Balasubramani, G. P. Chen, S. Coriani, M. Diedenhofen, M. S. Frank, Y. J. Franzke, F. Furche, R. Grotjahn, M. E. Harding, C. Hättig, A. Hellweg, B. Helmich-Paris, C. Holzer, U. Huniar, M. Kaupp, A. Marefat Khah, S. Karbalaei Khani, T. Müller, F. Mack, B. D. Nguyen, S. M. Parker, E. Perlt, D. Rappoport, K. Reiter, S. Roy, M. Rückert, G. Schmitz, M. Sierka, E. Tapavicza, D. P. Tew, C. Van Wüllen, V. K. Voora, F. Weigend, A. Wodyński, J. M. Yu, *J. Chem. Phys.* **2020**, *152*, 184107.

[9] D. Gallego, S. Inoue, B. Blom, M. Driess, *Organometallics* **2014**, *33*, 6885–6897.

[10] a) V. Y. Lee, T. Fukawa, M. Nakamoto, A. Sekiguchi, B. L. Tumanskii, M. Karni, Y. Apeloig, *J. Am. Chem. Soc.* **2006**, *128*, 11643–11651; b) D. E. Goldberg, P. B. Hitchcock, M. F. Lappert, K. M. Thomas, A. J. Thorne, T. Fjeldberg, A. Haaland, B. E. R. Schilling, *J. Chem. Soc. Dalton Trans.* **1986**, 2387–2394; c) M. Weidenbruch, H. Kilian, K. Peters, H. G. V. Schnering, H. Marsmann, *Chem. Ber.* **1995**, *128*, 983–985; d) H. Preut, H. J. Haupt, F. Huber, *Z. Anorg. Allg. Chem.* **1973**, *396*, 81–89; e) H. Jacobsen, T. Ziegler, *J. Am. Chem. Soc.* **1994**, *116*, 3667–3679; f) M. Weidenbruch, *J. Organomet. Chem.* **2002**, *646*, 39–52; g) U. Lay, H. Pritzkow, H. Grützmacher, *J. Chem. Soc. Chem. Commun.* **1992**, 260–262.

[11] a) J. P. Perdew, K. Burke, M. Ernzerhof, *Phys. Rev. Lett.* **1996**, *77*, 3865–3868; b) C. Adamo, V. Barone, *J. Chem. Phys.* **1999**, *110*, 6158–6170.

[12] F. Weigend, R. Ahlrichs, *Phys. Chem. Chem. Phys.* **2005**, *7*, 3297.

[13] J. M. Foster, S. F. Boys, *Rev. Mod. Phys.* **1960**, *32*, 300–302.

[14] J. Henning, K. Eichele, R. F. Fink, L. Wesemann, *Organometallics* **2014**, *33*, 3904–3918.

[15] a) S. S. Sen, M. P. Kritzler-Kosch, S. Nagendran, H. W. Roesky, T. Beck, A. Pal, R. Herbst-Irmer, *Eur. J. Inorg. Chem.* **2010**, 5304–5311; b) A. V. Zabula, T. Pape, A. Hepp, F. M. Schappacher, U. C. Rodewald, R. Pöttgen, F. E. Hahn, *J. Am. Chem. Soc.* **2008**, *130*, 5648–5649.

[16] a) D. Peng, N. Middendorf, F. Weigend, M. Reiher, *J. Chem. Phys.* **2013**, *138*, 184105; b) Y. J. Franzke, N. Middendorf, F. Weigend, *J. Chem. Phys.* **2018**, *148*, 104110; c) Y. J. Franzke, F. Weigend, *J. Chem. Theory Comput.* **2019**, *15*, 1028–1043; d) Y. J. Franzke, F. Mack, F. Weigend, *J. Chem. Theory Comput.* **2021**, *17*, 3974–3994; e) C. Holzer, Y. J. Franzke, A. Pausch, *J. Chem. Phys.* **2022**, *157*, 204102.; f) Y. J. Franzke, R. Treß, T. M. Pazdera, F. Weigend, *Phys. Chem. Chem. Phys.* **2019**, *21*, 16658–16664.

[17] a) A. D. Becke, *Phys. Rev. A* **1988**, *38*, 3098–3100; b) A. D. Becke, *J. Chem. Phys.* **1993**, *98*, 1372–1377; c) C. Lee, W. Yang, R. G. Parr, *Phys. Rev. B* **1988**, *37*, 785–789.

[18] a) J. Tao, J. P. Perdew, V. N. Staroverov, G. E. Scuseria, *Phys. Rev. Lett.* **2003**, *91*, 146401; b) V. N. Staroverov, G. E. Scuseria, J. Tao, J. P. Perdew, *J. Chem. Phys.* **2003**, *119*, 12129–12137.

[19] J.-D. Chai, M. Head-Gordon, *Phys. Chem. Chem. Phys.* **2008**, *10*, 6615.

[20] C. Holzer, Y. J. Franzke, *J. Chem. Phys.* **2022**, *157*, 034108.

[21] P. Pollak, F. Weigend, *J. Chem. Theory Comput.* **2017**, *13*, 3696–3705.

[22] A. V. Zabula, F. E. Hahn, *Eur. J. Inorg. Chem.* **2008**, 5165–5179.

[23] K. M. Krebs, S. Freitag, J. J. Maudrich, H. Schubert, P. Sirsch, L. Wesemann, *Dalton Trans.* **2018**, *47*, 83–95.

[24] A. E. Reed, R. B. Weinstock, F. Weinhold, *J. Chem. Phys.* **1985**, *83*, 735–746.

[25] R. S. Mulliken, *J. Chem. Phys.* **1955**, *23*, 1833–1840.

[26] O. Altintas, E. Lejeune, P. Gerstel, C. Barner-Kowollik, *Polym. Chem.* **2012**, *3*, 640–651.

[27] a) R. Jambor, L. Dostál, M. Erben, Z. Růžičková, R. Jirásko, A. Hoffmann, *Organometallics* **2021**, *40*, 783–791; b) P. B. Hitchcock, M. F. Lappert, L. J. M. Pierssens, *Organometallics* **1998**, *17*, 2686–2688.

[28] a) M. Dahlen, M. Kehry, S. Lebedkin, M. M. Kappes, W. Klopper, P. W. Roesky, *Dalton Trans.* **2021**, *50*, 13412–13420; b) M. Dahlen, E. H. Hollesen, M. Kehry, M. T. Gamer, S. Lebedkin, D. Schooss, M. M. Kappes, W. Klopper, P. W. Roesky, *Angew. Chem.* **2021**, *133*, 23553–23560; *Angew. Chem. Int. Ed.* **2021**, *60*, 23365–23372; c) M. Dahlen, T. P. Seifert, S. Lebedkin, M. T. Gamer, M. M. Kappes, P. W. Roesky, *Chem. Commun.* **2021**, *57*, 13146–13149.

[29] a) F. Furche, D. Rappoport, *Theor. Comput. Chem.*, Elsevier, Amsterdam, **2005**, 93; b) R. Bauernschmitt, R. Ahlrichs, *Chem. Phys. Lett.* **1996**, *256*, 454–464; c) M. Sierka, A. Hogekamp, R. Ahlrichs, *J. Chem. Phys.* **2003**, *118*, 9136–9148; d) R. Bauernschmitt, M. Häser, O. Treutler, R. Ahlrichs, *Chem. Phys. Lett.* **1997**, *264*, 573–578.

[30] F. Furche, R. Ahlrichs, *J. Chem. Phys.* **2002**, *117*, 7433–7447.

[31] a) V. Phillips, K. J. Willard, J. A. Golen, C. J. Moore, A. L. Rheingold, L. H. Doerrer, *Inorg. Chem.* **2010**, *49*, 9265–9274; b) V. Phillips, F. G. Baddour, T. Lasanta, J. M. López-de-Luzuriaga, J. W. Bacon, J. A. Golen, A. L. Rheingold, L. H. Doerrer, *Inorg. Chim. Acta* **2010**, *364*, 195–204.

Manuscript received: November 17, 2022
Accepted manuscript online: December 19, 2022
Version of record online: ■■, ■■■

RESEARCH ARTICLE

Tin shines better with gold or silver: A luminescent pincer-type bis-stannylene ligand for exclusive tetrahedral coordination of the coinage metals was designed, and photoluminescence investigations as well as extensive quantum chemical calculations were carried out.

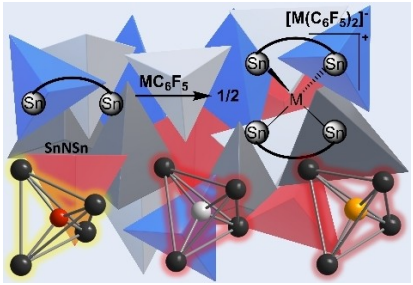

*F. Krätschmer, Dr. X. Sun, S. Gillhuber, H. Kucher, Dr. Y. J. Franzke, Prof. Dr. F. Weigend, Prof. Dr. P. W. Roesky**